
PERSONALIZED FEDERATED LEARNING VIA SEQUENTIAL LAYER EXPANSION IN REPRESENTATION LEARNING

Jaewon Jang, Bonjun Choi
Computer Science and Engineering
Soongsil University
Seoul, South Korea
{jwon0524, davidchoi}@soongsil.ac.kr

ABSTRACT

Federated learning ensures the privacy of clients by conducting distributed training on individual client devices and sharing only the model weights with a central server. However, in real-world scenarios, the heterogeneity of data among clients necessitates appropriate personalization methods. In this paper, we aim to address this heterogeneity using a form of parameter decoupling known as representation learning. Representation learning divides deep learning models into 'base' and 'head' components. The base component, capturing common features across all clients, is shared with the server, while the head component, capturing unique features specific to individual clients, remains local. We propose a new representation learning-based approach that suggests decoupling the entire deep learning model into more densely divided parts with the application of suitable scheduling methods, which can benefit not only data heterogeneity but also class heterogeneity. In this paper, we compare and analyze two layer scheduling approaches, namely forward (*Vanilla*) and backward (*Anti*), in the context of data and class heterogeneity among clients. Our experimental results show that the proposed algorithm, when compared to existing personalized federated learning algorithms, achieves increased accuracy, especially under challenging conditions, while reducing computation costs.

Keywords Federated Learning · Personalized Federated Learning · Representation Learning · data heterogeneity

1 Introduction

Traditional centralized machine learning collects all raw data to a central server for training. However, concerns about data privacy have grown among companies and researchers in the era of big data. Moreover, the implementation of stringent legal regulations, such as the General Data Protection Regulation (GDPR) [1] in Europe and the California Consumer Privacy Act (CCPA) [2] in the United States, has underscored the need for new methods of collecting and sharing client data that comply with these laws. In this context, federated learning has emerged as a significant research area, allowing the utilization of diverse data distributed across various devices like smartphones, IoT devices, and wearables while ensuring data privacy.

Federated learning [3], in contrast to centralized machine learning, does not directly share raw client data with a central server. Instead, it trains models on each edge device and shares only the model's weights, aggregating them to update a global model. This training approach ensures privacy, as raw data is not shared with the server, and it offers communication cost advantages when dealing with large datasets. However, in real-world scenarios, local data among clients can be highly heterogeneous, exhibiting varying data distributions. This heterogeneity can lower the performance of the global model during server-side aggregation and may introduce bias towards certain clients.

Therefore, the need for suitable personalization methodologies arises to capture and optimize each client's unique data characteristics. To address these issues, personalized federated learning (PFL) approaches [4, 5] are actively being researched. In this study, we utilize representation learning which is one of the PFL approaches. Representation learning divides the layers of a deep learning model into *base* and *head* components. In representation learning, the *base* (or

feature extractor) part represents common features for all clients and is shared with the server and all clients. The *head (or classifier)* part represents unique features for specific clients and remains on the local device, not shared with the server. Typically, the *head* part uses the last fully connected layer (classification layer), and in our experimental setup, we also designate the *head* part as the last fully connected layer while setting the remaining layers as the *base* part.

Our idea originated with the goal of subdividing the components of the deep learning model in representation learning more densely than just the base and head. Additionally, the layer scheduling approach drew inspired from curriculum learning [6], resulting in the development of both Vanilla and Anti scheduling.

Curriculum learning is a method that, similar to how human learning, gradually progresses from easy examples to more challenging ones. Traditional curriculum learning focuses on determining the difficulty of datasets and utilizes pre-trained expert models on the entire dataset to evaluate the difficulty of each data point. Subsequently, it assigns difficulty scores based on the client’s loss using the pre-trained expert model and then conducts training either by starting with easy examples and progressing to harder ones or vice versa. In the recently researched federated learning environment, curriculum learning [7] also necessitates a well-trained expert model.

However, curriculum learning relies on expert models to assess the difficulty of data points. This dependence can result in significantly reduced performance if the expert models are compromised by malicious attacks or poorly trained. Furthermore, the process of assigning difficulty scores and dividing datasets based on difficulty can complicate operations in a federated learning environment, as highlighted by [7]. In contrast to curriculum learning, our scheduling algorithm does not categorize data based on difficulty levels. Instead, it focuses on decoupling layers according to the principles of representation learning. In typical deep learning models, the initial layers are responsible for extracting low-level features, while the later layers handle the extraction of more complex and abstract features. Building on this insight, we have concentrated on more densely separating the base layer in representation learning algorithms and sequentially training it, deviating from the traditional curriculum learning approach.

Hence, our algorithm densely divides the base layer, initially freezing the entire layer set, and then progressively unfreezes specific layers for training according to a schedule. There are two scheduling methods: *Vanilla* scheduling, which starts by unfreezing layers closest to the input and progresses towards the output, and *Anti* scheduling, which begins by unfreezing layers nearest to the output and works backward. A key advantage of our proposed algorithm is that, during the early rounds, only a portion of the unfrozen base layer is shared with the server, rather than the entirety. This approach not only enhances performance but also reduces the communication and computational costs compared to other algorithms.

The contributions of this paper are as follows:

- Our algorithm densely divides the base layer to address the heterogeneity of the client’s data and class distribution, and it proposes two scheduling methods.
- The implementation of scheduling reduces the need to communicate all base layers in the early stages of training, thereby cutting down on communication and computational costs.
- In scenarios with both data and class heterogeneity, the *Anti* scheduling approach outperforms other algorithms in terms of accuracy, while the *Vanilla* scheduling method significantly reduces computational costs compared to other algorithms.
- We visually present the accuracy for each client and mathematically compare the computational costs of each algorithm.

2 Related Work

2.1 Federated Learning

Federated Learning is a machine learning technique that enables training while ensuring the privacy of clients’ distributed data [3]. However, a significant challenge in real-world federated learning scenarios is the heterogeneity of the data distribution among distributed clients, necessitating the application of appropriate personalization techniques.

2.2 Personalized Federated Learning

Personalized Federated Learning (PFL) has been proposed to tackle the heterogeneity of client data and can be categorized into several approaches such as Clustering, Meta Learning, and Representation [8]. This section compares three related personalization methods, including representation learning, which are considered similar.

2.2.1 Meta Learning

Meta learning, also referred to as learning to learn, was initially proposed for few-shot learning. [9] focuses on finding model initialization methods that can rapidly adapt to new and unseen tasks, allowing for the quick learning of new tasks with limited data. [10] employs first-order algorithms, which are computationally less complex compared to other meta-learning algorithms, and demonstrates comparable performance without the need for second-order methods.

2.2.2 Transfer Learning

Transfer learning has also been proposed for few-shot learning and is a method to apply knowledge learned in a specific domain to a different domain. It involves adapting a pre-trained backbone from a different domain to a similar but distinct domain using the well-known method of fine-tuning. [11] helps solve heterogeneity by transferring and learning knowledge between models with different structures. Additionally, [12] proposes a federated transfer learning framework for wearable health data.

2.2.3 Multi-task Learning

Multi-task learning is a method that can enhance a model’s generalization ability by simultaneously learning multiple tasks and sharing knowledge or representations between these tasks. In [13], a novel approach is proposed that combines federated learning with multi-task learning. This approach improves the performance of each task by addressing multiple related learning tasks simultaneously, enabling efficient learning through the utilization of shared knowledge.

2.2.4 Representaion Learning

The PFL technique we used is a kind of representation learning, which is a parameter decoupling method to alleviate statistical heterogeneity. Representation learning is a method of training deep learning models by dividing the layers into a base and a head. The base shares common features among clients, while the head layer keeps in locally and is used for personalization [14].

Moreover, [15] argues that it generalizes more easily to new devices compared to other learning mechanisms and that fair representations, which obscure protected attributes, are effectively learned through adversarial training. Additionally, [16] demonstrates fast convergence in linear regression problems by leveraging distributed computational power among clients to perform many local updates. Furthermore, [17] shows that there is a discrepancy in the validation methods between general federated learning algorithms and personalized federated learning algorithms. They argue that both local and global model accuracy should be considered and introduce a new loss function to mitigate class imbalance issues. In addition, [18] suggests that updating the head in cases where client data is highly heterogeneous can negatively affect personalization. Therefore, during training rounds, a randomly initialized head is used, employing only the body for training and aggregation. We adopt a similar training setup [18], using a randomly initialized head during training rounds, and the head is only utilized in the final fine-tuning after the training rounds are completed.

3 Proposed Algorithm

Table 1: List of Symbols Used

Symbol	Description
N	Total number of clients
C_i	Client i , $i \in \{1, 2, \dots, N\}$
$ D_i $	Number of data points for client i
$ D $	Total number of data points
T	Total global rounds
F	Fine-tuning rounds
K	Total number of base layers
t_k	Unfreeze point (round) of k -th layer
η	Learning Rate
\mathcal{L}	Loss Function
θ_i	Local parameter for client i
θ_G	Global model parameter
$\theta_{i,b}$	Base parameter shared among all clients
$\theta_{i,p}$	Head parameter of client i

In this section, we present our proposed algorithms in detail, namely *Vanilla Scheduling* and *Anti Scheduling*. As shown in Figure 1, Vanilla Scheduling starts by unfreezing the shallowest layers (closest to the input) and progressively moves towards deeper layers. This method allows the model to capture low-level features early in the training process, which is crucial for building a strong foundational understanding before more high-level features are introduced. Conversely, Anti Scheduling begins with the deepest layers (closest to the output) and progressively unfreezes towards the input. This approach prioritizes the learning of high-level features from the outset, which can be beneficial for complex pattern recognition tasks that depend heavily on such features.

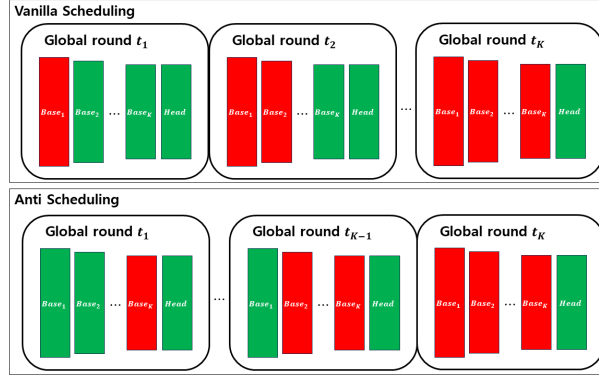


Figure 1: Illustration of the proposed Vanilla and Anti Scheduling algorithms. The upper shows Vanilla Scheduling, starting with the shallowest layer and advancing to deeper ones. The lower shows Anti Scheduling, which begins with the deepest layer and progresses inversely.

As shown in Figure 1, the structured progression from shallow to deep layers in Vanilla Scheduling, and the reverse in Anti Scheduling, structurally differ from traditional representation learning. In traditional representation learning methods, the base and head of the model are typically trained simultaneously without specific layer prioritization. In our approach, however, each layer’s training is specifically timed and prioritized. This strategic scheduling enhances the model’s ability to adapt to varying complexities of features throughout the training process.

Furthermore, as detailed in Section 5.2, Vanilla Scheduling can achieve comparable accuracy with significantly lower computational costs in environments characterized by high data and class heterogeneity. In contrast, Anti Scheduling excels in achieving the highest accuracy in scenarios where both data and class heterogeneity are pronounced. They both follow the basic federated learning setup and the representation learning as explained below.

As a basic federated learning setup, we assume that each client C_i possess data $\mathbf{D}_i = (x_i, y_i) \in R^d$, where $i \in 1, 2, \dots, N$ represents i -th client out of a total of N clients and d represents the input dimension. Each client i updates its local model parameter θ_i based on its data D_i and the global model parameter θ_G as

$$\theta_i^{(t+1)} = \theta_i^{(t)} - \eta \nabla_{\theta_i} \mathcal{L}(D_i, \theta_i^{(t)}), \quad (1)$$

where η is the learning rate, ∇L is the gradient of the loss function L , and $t \in (1, 2, \dots, T)$ denotes the number of rounds. The central server updates the global parameter θ_G based on all clients’ local parameter updates as

$$\theta_G^{(t+1)} = \sum_{i=1}^N \frac{|D_i|}{|D|} \theta_i^{(t+1)}, \quad (2)$$

where $|D_i|$ is the number of data points for client i , and $|D|$ is the total number of data points.

For representation learning, the model parameters are divided into two components $\theta_i = (\theta_{i,b}, \theta_{i,h})$. Here, $\theta_{i,b}$ represents the base parameter shared among all clients and $\theta_{i,h}$ represents the head parameter of the i -th client. The model parameters from Eq. (1) is modified as follows:

$$\theta_i^{(t+1)} = \theta_i^{(t)} - \eta \nabla_{\theta_i} \mathcal{L}(D_i, \theta_{i,b}^{(t)}, \theta_{i,h}^{(0)}). \quad (3)$$

Excluding FedBABU [18], previous works the gradient of the head parameter is stopped during training and during the aggregation phase. The global model is updated using both the base and head parameters. However, FedBABU and our

scheduling algorithm perform both training and aggregation using only the base without involving the head. Only after training, a few rounds of fine-tuning are included using both the base and head.

The aggregation process, which excludes the use of the head, proceeds as follows:

$$\theta_G^{(t+1)} = \sum_{i=1}^N \frac{|D_i|}{|D|} \theta_{i,b}^{(t+1)}. \quad (4)$$

Our algorithm follows the same training setup as FedBABU [18], wherein the head layer is not trained or aggregated during training; instead, it is fine-tuned for each client after training completion. In FedBABU, the training round sets the learning rate of the head to zero, allowing gradient computation but preventing its application. In contrast, our scheduling algorithm ensures complete decoupling by freezing gradients in both the head and base parts, preventing both computation and application.

3.1 Method 1: Vanilla Scheduling

Vanilla scheduling is a training method that starts by thoroughly learning the shallowest layers (closest to the input) in the base layer, freezing the rest layers, and then progressively unfreezing them. This enables the model to preferentially learn low-level features and patterns, aiding in better understanding the abstract characteristics and patterns of the data. The training steps of Vanilla scheduling, which starts with the shallowest layers, can be represented as

$$\begin{aligned} \theta_i^{(t_1+1)} &= \theta_i^{(t_1)} - \eta \nabla_{\theta_i} \mathcal{L}(D_i, \theta_{i,b_1}^{(t_1)}, \theta_{i,b_2}^{(0)}, \dots, \theta_{i,b_{K-1}}^{(0)}, \theta_{i,b_K}^{(0)}, \theta_{i,h}^{(0)}) \\ \theta_i^{(t_2+1)} &= \theta_i^{(t_2)} - \eta \nabla_{\theta_i} \mathcal{L}(D_i, \theta_{i,b_1}^{(t_2)}, \theta_{i,b_2}^{(t_2)}, \dots, \theta_{i,b_{K-1}}^{(0)}, \theta_{i,b_K}^{(0)}, \theta_{i,h}^{(0)}) \\ &\vdots \\ \theta_i^{(t_K+1)} &= \theta_i^{(t_K)} - \eta \nabla_{\theta_i} \mathcal{L}(D_i, \theta_{i,b_1}^{(t_K)}, \theta_{i,b_2}^{(t_K)}, \dots, \theta_{i,b_{K-1}}^{(t_K)}, \theta_{i,b_K}^{(0)}, \theta_{i,h}^{(0)}). \end{aligned} \quad (5)$$

In Eq. (5), Once the first base layer θ_{i,b_1} is sufficiently trained, the freeze on the next base layer θ_{i,b_2} is released for training. This sequential unfreezing and training of base layers up to θ_{i,b_K} defines Vanilla scheduling. The $\{t_1, t_2, \dots, t_K \in T\}$ represent the global rounds where the freeze of each layer is released. Throughout the training process, the head layer $\theta_{i,h}$ is initialized and kept frozen, only being utilized in the final fine-tuning stage.

3.2 Method 2: Anti Scheduling

Anti scheduling is a training approach that initiates with the deepest layers (closest to the output) in the base layer, freezing the remaining layers, and then progressively unfreezing them for sufficient training. This method allows the model to preferentially grasp high-level and various features. The training steps of Anti scheduling, starting with the deepest layers, can be given as

$$\begin{aligned} \theta_i^{(t_1+1)} &= \theta_i^{(t_1)} - \eta \nabla_{\theta_i} \mathcal{L}(D_i, \theta_{i,b_1}^{(0)}, \theta_{i,b_2}^{(0)}, \dots, \theta_{i,b_{K-1}}^{(0)}, \theta_{i,b_K}^{(t_1)}, \theta_{i,h}^{(0)}) \\ \theta_i^{(t_2+1)} &= \theta_i^{(t_2)} - \eta \nabla_{\theta_i} \mathcal{L}(D_i, \theta_{i,b_1}^{(0)}, \theta_{i,b_2}^{(0)}, \dots, \theta_{i,b_{K-1}}^{(t_2)}, \theta_{i,b_K}^{(t_2)}, \theta_{i,h}^{(0)}) \\ &\vdots \\ \theta_i^{(t_K+1)} &= \theta_i^{(t_K)} - \eta \nabla_{\theta_i} \mathcal{L}(D_i, \theta_{i,b_1}^{(t_K)}, \theta_{i,b_2}^{(t_K)}, \dots, \theta_{i,b_{K-1}}^{(t_K)}, \theta_{i,b_K}^{(t_K)}, \theta_{i,h}^{(0)}). \end{aligned} \quad (6)$$

In Eq (6), once the deepest base layer θ_{i,b_K} is sufficiently trained, the freeze on the preceding layer $\theta_{i,b_{K-1}}$ is released for training. Anti scheduling is thus defined as the sequential unfreezing and training of base layers starting from θ_{i,b_K} and proceeding to the first base layer θ_{i,b_1} . The training progresses in the reverse order of Anti scheduling, and during this process, the head layer $\theta_{i,h}$ remains frozen and is only utilized in the final fine-tuning phase.

Algorithm 1 outlines the training procedure for both Vanilla and Anti scheduling. Line 2 represents client sampling. Lines 4–8 represent the Vanilla scheduling mode. When the Vanilla mode is selected, if the current global round t is greater than the layers unfreeze round t_k , as specified in line 5, the algorithm unfreezes the k -th base parameter θ_{i,b_k} . Then, in line 8, the unfrozen base parameters are used to perform a local update.

Algorithm 1 Layer Decoupling Algorithm with Vanilla and Anti Scheduling

Input: Total global rounds T , Total clients N , join ratio r , Learning rate η , Total base layers K , Fine-tuning rounds F , Scheduling Mode $Mode$, Layer Unfreeze Rounds t_1, t_2, \dots, t_K

Initialize: Global base parameters $\theta_{G,b_1}^{(0)}, \theta_{G,b_2}^{(0)}, \dots, \theta_{G,b_K}^{(0)}$ and Global Head parameter $\theta_{G,h}^{(0)}$

```

1: for  $t = 1$  to  $T$  do
2:   Randomly select  $M = \lfloor r \times N \rfloor$  clients
3:   for Each selected client  $i = 1$  to  $M$  do
4:     if  $Mode = 'Vanilla'$  then
5:       if  $t \geq t_k$  then
6:         Unfreeze  $\theta_{i,b_k}$ 
7:       end if
8:        $\theta_i^{(t+1)} = \theta_i^{(t)} - \eta \nabla_{\theta_i} \mathcal{L}(D_i, \theta_{i,b_1}^{(t)}, \dots, \theta_{i,b_K}^{(t)}, \theta_{i,h}^{(0)})$ 
9:     else if  $Mode = 'Anti'$  then
10:      if  $t \geq t_k$  then
11:        Unfreeze  $\theta_{i,b_{K-k+1}}$ 
12:      end if
13:       $\theta_i^{(t+1)} = \theta_i^{(t)} - \eta \nabla_{\theta_i} \mathcal{L}(D_i, \theta_{i,b_1}^{(t)}, \dots, \theta_{i,b_K}^{(t)}, \theta_{i,h}^{(0)})$ 
14:    end if
15:    Keep  $\theta_{i,h}$  frozen
16:    Send updated base parameters  $\theta_{i,b_1}^{(t+1)}, \dots, \theta_{i,b_K}^{(t+1)}$ 
17:  end for
18:  Aggregate global model  $\theta_G^{(t+1)} = \sum_{i=1}^N \frac{|D_i|}{|D|} \theta_{i,b}^{(t+1)}$ 
19: end for
20: for  $f = 1$  to  $F$  do
21:   Unfreeze all layers for each client
22:   for each client  $i = 1$  to  $N$  do
23:    Update all parameters  $\theta_i$  for fine tuning
24:     $\theta_i^{(T+f)} = \theta_i^{(T+f-1)} - \eta \nabla_{\theta_i} \mathcal{L}(D_i, \theta_{i,b_1}^{(T+f-1)}, \dots, \theta_{i,b_K}^{(T+f-1)}, \theta_{i,h}^{(T+f-1)})$ 
25:   end for
26: end for
    
```

Lines 9–13 describe the Anti scheduling mode. In Anti mode, as line 10 indicates, if the current global round t exceeds the layer unfreeze round t_k , the algorithm unfreezes the $(K - k + 1)$ -th base parameter $\theta_{i,b_{K-k+1}}$, which is closer to the head layer. Line 13 then uses the unfrozen base parameters for the local update. Lines 15–16 maintain the freezing of the head while sending the updated base parameters to the server. Line 18 performs global aggregation after local updates, and lines 20–24 is the fine-tuning process in which both base and head parameters are utilized in each client after the global rounds are complete

4 Experiments

In our experimental setup, the total number of clients N is set to 100, with each round involving a client participation ratio r of 0.1, indicating that 10 clients participate in each training round. The batch size is configured to 10, and the learning rate is set at 0.005. The datasets used in our experiments include MNIST, CIFAR-10, CIFAR-100, and Tiny-ImageNet. To induce heterogeneity among the data distributed to each client, we sampled from a Dirichlet distribution with a Dirichlet parameter of 0.1, establishing a highly heterogeneous environment. This approach to data distribution is visualized in Figure 2, which illustrates the results of sampling the CIFAR-10 dataset among 10 clients. Despite the high heterogeneity induced by the Dirichlet parameter α of 0.1, MNIST and CIFAR-10 dataset inherently lacks significant class heterogeneity. Therefore, our experiments focus on CIFAR-100 and Tiny-ImageNet datasets because our approach performs well in environments with significant data and class heterogeneity. The CIFAR-100 dataset contains 100 different classes, and the Tiny-ImageNet dataset contains 200 classes.

In our experiments, we compare our approach against six baselines, as detailed in the following references: [14, 17, 16, 15, 3, 18]. The model used is a shallow CNN model comprising two convolutional layers and two fully connected layers. Here, the last fully connected layer is set as the *head*, and the remaining three layers are designated as the base. The total number of base layers K is set to 3, with t_1 at the 0 (initial) round, t_2 at the 100-th global round, and

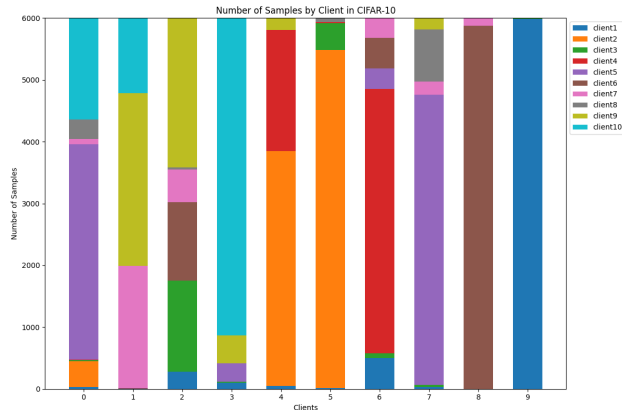


Figure 2: Results of sampling the CIFAR-10 dataset among 10 clients from a Dirichlet distribution. The Dirichlet parameter α is 0.1, generating highly heterogeneous data. However, the nature of the CIFAR-10 dataset does not offer much class heterogeneity.

t_3 at the 200-th global round. Additionally, in FedBABU [18], the learning rate of the *head* is set to zero during the training rounds, implying that gradients are calculated but not applied. In contrast, our scheduling algorithm achieves complete decoupling by freezing the gradients, thus preventing both computation and application. We will delve into the comparison of computational and communication costs in Section 5.2.

Table 2: Comparison of accuracy

Algorithm	MNIST		CIFAR-10		CIFAR-100		Tiny-ImageNet	
	Acc. (%)	T	Acc. (%)	T	Acc. (%)	T	Acc. (%)	T
FedAvg [3]	91.48	100	36.87	100	29.04	500	16.97	300
	96.32	200	42.00	200	30.95	1000	14.06	500
	97.48	300	49.36	300	30.34	1500	14.27	1500
FedPer [14]	98.30	100	86.16	100	40.22	500	29.04	300
	98.63	200	87.34	200	41.03	1000	29.24	500
	98.69	300	86.66	300	40.05	1500	29.11	1000
LG-FedAvg [15]	97.95	100	85.75	100	41.06	500	26.46	300
	98.17	200	86.10	200	41.01	1000	26.35	500
	98.13	300	85.91	300	40.80	1500	26.36	1000
FedRep [16]	98.56	100	86.58	100	40.44	500	28.85	300
	98.69	200	88.12	200	41.24	1000	28.54	500
	98.75	300	88.11	300	40.66	1000	28.50	1000
FedROD [17]	98.61	100	86.24	100	49.50	500	37.23	300
	98.95	200	88.01	200	48.70	1000	35.34	500
	99.06	300	88.59	300	50.56	1500	35.35	1000
FedBABU [18]	98.19	100	85.77	100	49.28	500	37.84	300
	98.77	200	86.16	200	52.75	1000	33.78	500
	98.84	300	87.07	300	51.82	1500	32.57	1000
Vanilla Scheduling	98.21	100	85.82	100	56.86	500	41.86	300
	98.84	200	87.81	200	59.52	1000	39.51	500
	98.99	300	88.58	300	58.49	1500	36.44	1000
Anti Scheduling	98.34	100	85.73	100	56.17	500	41.94	300
	98.81	200	87.67	200	60.06	1000	39.67	500
	98.96	300	88.61	300	58.58	1500	36.63	1000

Table 2 presents a comparison of the accuracies achieved by various federated learning algorithms across multiple datasets, including MNIST, CIFAR-10, CIFAR-100, and Tiny-ImageNet. It encompasses representation learning algorithms such as FedAvg, FedPer, LG-FedAvg, FedRep, FedROD, and FedBABU, as well as our proposed Vanilla and Anti scheduling algorithms. A key aspect of both FedBABU and our scheduling algorithms is their approach during the training phases leading up to the final global round, denoted as T . Characteristically, these algorithms exclusively use the base layers and do not employ the head layer during the training rounds, resulting in relatively lower accuracies prior to the final round. To ensure a fair comparison, the accuracy figures for FedBABU and our scheduling algorithms at T represent the performance after fine-tuning. Additionally, it is noteworthy that our scheduling algorithms have achieved high accuracy in environments with significant data and class heterogeneity, demonstrating their effectiveness in processing complex and diverse datasets.

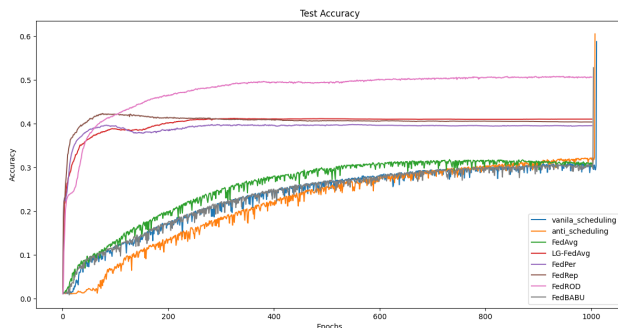


Figure 3: This figure shows the average accuracy of clients on the CIFAR-100 dataset. As can be seen, the earlier round accuracy of our scheduling algorithm is lower than FedAvg and FedBABU. This is because, in the earlier rounds, not all base and head participate and the training is conducted using only a portion of the unfrozen base layers.

Figure 3 shows the average accuracy of clients on the CIFAR-100 dataset, visualizing the performance of our scheduling algorithms compared to baselines. As can be seen, the earlier round accuracy of our scheduling algorithm is lower than FedAvg and FedBABU, which is attributed to the fact that, in the earlier rounds, not only all base but also head participate, and the training is conducted using only a portion of the unfrozen base layers.

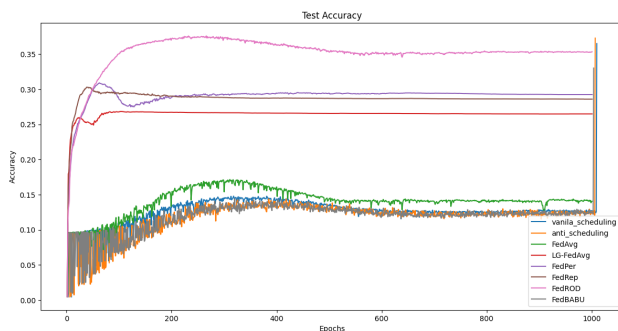


Figure 4: This figure represents the average accuracy of clients on the Tiny-ImageNet dataset, where the initial round accuracy of our scheduling algorithm is lower compared to FedAvg and FedBABU, consistent with its characteristics.

Similarly, Figure 4 represents the average accuracy of clients on the Tiny-ImageNet dataset. Our scheduling algorithm’s earlier round accuracy is lower than FedAvg and FedBABU, consistent with its characteristics. This visualization helps underscore how our scheduling algorithms gradually catch up and potentially surpass other algorithms as the training progresses.

5 Ablation Study

In our ablation study, we demonstrate the results of varying different parameters. The contents to be covered in the ablation study include:

- Comparison of client-specific accuracy

- Estimation of computational cost for each algorithm
- Effect of layer unfreezing timing on the accuracy
- Application of scheduling to the baseline algorithms

5.1 Comparison of Client-specific Accuracy

To ensure that accuracy improvements during fine-tuning are not biased or limited to specific clients, we conducted a comparative analysis of client-specific accuracy between the latest representation learning algorithms and our algorithm. Since the accuracy differences in the MNIST and CIFAR-10 datasets are not significantly pronounced, the comparison was focused on the CIFAR-100 and Tiny-ImageNet datasets. The results demonstrated that the higher average accuracy of our scheduling algorithm was not due to bias towards specific clients but was consistently achieved across all clients.

Figure 5 shows the comparison of client-specific accuracy in the CIFAR-100 dataset. This visualization helps to highlight that our scheduling algorithm achieves consistent accuracy across a spectrum of different clients without favoring any particular group.

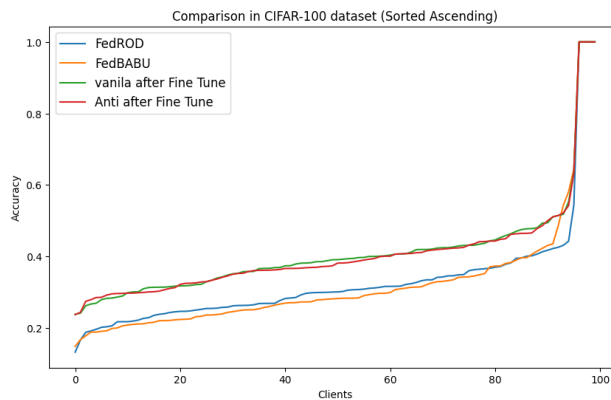


Figure 5: Comparison of client-specific accuracy in the CIFAR-100 dataset. This figure visualizes the accuracy of each client in ascending order.

Similarly, Figure 6 demonstrates the client-specific accuracy in the Tiny-ImageNet dataset. As with CIFAR-100, the visualization confirms that our algorithm manages to maintain high accuracy uniformly across different clients, showcasing its robustness.

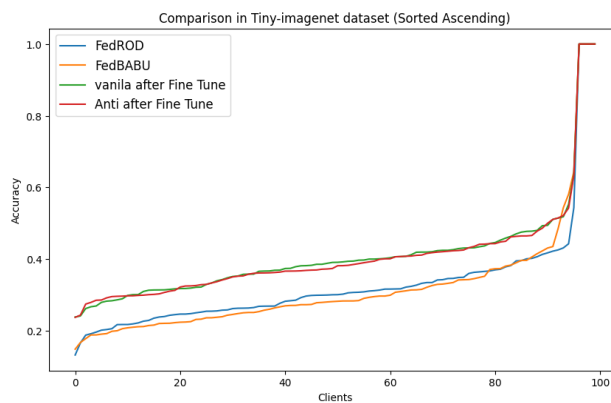


Figure 6: Comparison of client-specific accuracy in the Tiny-ImageNet dataset. This figure visualizes the accuracy of each client in ascending order.

5.2 Estimation of Computational Cost for Each Algorithm

In the actual experimental environment, using non-IID data makes it challenging to estimate computational costs. Therefore, we estimate the computational costs using the number of FLOPs. The number of parameters in each layer is mentioned following in Table 3.

Table 3: Number of Parameter per Layer

Layer	# of Parameters
conv1.weight	800
conv1.bias	32
conv2.weight	51,200
conv2.bias	64
fc1.weight	524,288
fc1.bias	512
fc2.weight	5,120
fc2.bias	10
Total Parameters	582,026

To compare the computational costs of FedAvg, FedBABU, and our scheduling algorithms, we consider the data processed by each client in an IID (independent and identically distributed) environment. Costs are measured in FLOPs, and for simplicity, all algorithms are assumed to use datasets with an equal pixel count per image. In datasets like MNIST, CIFAR-10, and CIFAR-100, each with a total of 50,000 training data and 100 clients, each client processes 500 data points. In the setting of our experiments, a batch size of 10 is used, with each client handling 50 batches per epoch.

For FedAvg, as seen in the Table 3, the total model parameters are 582,026, and the computational cost per round is $582,026 \times 50$. Thus, the total computational cost for all clients and all rounds is 873.039 billion FLOPs. In the same environment, the computational cost for FedBABU, considering that the *head* (fc2) layer parameters are not computed during the training rounds, results in 576,896 learning parameters. Hence, the total computational cost for FedBABU is 865.344 billion FLOPs. Using the same method for our scheduling algorithms, the computed parameters result in 314.912 billion FLOPs for Vanilla Scheduling and 838.880 billion FLOPs for Anti Scheduling, as detailed in Table 4.

Figure 7 visually compares the computational costs between FedAvg, FedBABU, and our scheduling algorithms. It illustrates how Vanilla scheduling significantly reduces computational costs in the earlier rounds by updating only the earlier unfreezed layers. This visualization supports the data presented in Table 4, emphasizing the efficiency of Vanilla Scheduling in managing computational resources.

Table 4: Comparison of Computational Cost

Algorithm	# of FLOPs ($\times 10^9$)	T
FedAvg [3]	873,04	300
FedBABU [18]	865,34	300
Vanilla Scheduling	314,91	300
Anti Scheduling	838,88	300

5.3 Accuracy Differences Due to Changes in Layer Unfreezing Timing

In our two scheduling algorithms, the number of base layers, t_k , is set to 3, leading to parameter unfreezing occurring across three phases. For instance, in Vanilla scheduling, training proceeds with the unfreezing of the conv1 layer from round $T = 0$ to 100. Subsequently, from rounds 100 to 200, both conv1 and conv2 layers are unfrozen for training. Finally, from round 200 to the final global round, all base layers, including conv1, conv2, and fc1, are unfrozen and utilized for training. While the unfreezing points in this paper are arbitrarily set for discussing the effectiveness of layer decoupling, an appropriate scheduling method is required accordingly. Therefore, we compare the differences in outcomes when unfreezing occurs at rounds 50 and 100 instead of 100 and 200.

In the CIFAR-100 dataset, with the global round $T = 1000$ and layer unfreezing round set at $t_1 = 0, t_2 = 100, t_3 = 200$, Vanilla scheduling achieves an accuracy of 59.52%, while Anti scheduling achieves 60.06%. However, when the unfreezing round is changed to $t_1 = 0, t_2 = 50, t_3 = 100$, Vanilla scheduling achieves 58.68%, and Anti scheduling achieves 59.02% accuracy, slightly lower accuracy. For the Tiny-ImageNet dataset at global round $T = 300$, with $t_1 = 0, t_2 = 100, t_3 = 200$, Vanilla and Anti scheduling achieve accuracies of 41.86% and 41.94%, respectively. Changing the unfreezing points to $t_1 = 0, t_2 = 50, t_3 = 100$ results in accuracies of 41.23% for Vanilla and 41.63% for

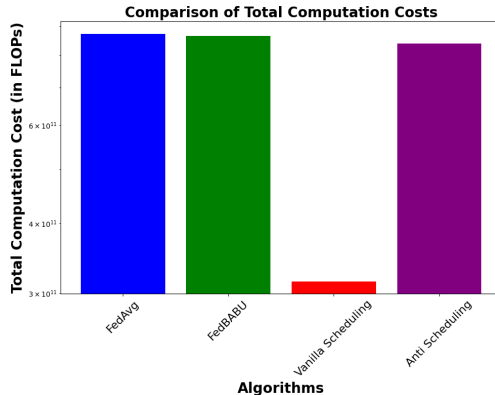


Figure 7: Comparison of computational costs between FedAvg, FedBABU, and our scheduling algorithms. Vanilla scheduling significantly reduces computational costs in the initial rounds by updating only the front-end layers.

Anti scheduling, which are also slightly lower. The insight gained here is that while the timing of layer unfreezing does not significantly affect accuracy, as seen in Section 5.2, it has a substantial impact on computational cost. Therefore, setting larger values for t_k is advantageous where possible.

5.4 Application of Scheduling to Baseline Algorithms

When our scheduling methods are applied to the baseline algorithms, there was no observed improvement in accuracy. This lack of improvement is attributed to the fact that, except for [18], other algorithms update the head during training rounds, which nullifies the effect of freezing base layers. Furthermore, Vanilla scheduling achieved a performance similar to the non-scheduled approach, while Anti scheduling, in particular, resulted in significantly lower accuracy. Therefore, natively applying a dense division of the base layer only for scheduling purposes might inadvertently lead to a negative impact on accuracy. Additionally, if the head layer is utilized for local updates during training, the intended effect of freezing the base layers is effectively nullified.

6 Conclusion

This research introduces a layer decoupling technique in representation learning, a domain of personalized federated learning, to address data and class heterogeneity among clients. In traditional representation learning, the model is divided into 'base' and 'head' components, each customized to process the common and unique features of client data, respectively. Our primary contribution focuses on the dense division of the base component in representation learning, and the subsequent application of two novel scheduling methodologies, namely Vanilla and Anti scheduling, to these finely segmented base layers in federated learning architecture. The Vanilla scheduling approach excels in significantly reducing computational costs without degrading model performance. This aspect is particularly crucial in federated learning environments where resources and computational power are often limited. Conversely, Anti scheduling demonstrates superior capability in handling scenarios with pronounced data and class heterogeneity. Our experimental analysis, conducted on datasets with high data and class heterogeneity, such as CIFAR-100 and Tiny-ImageNet, shows that these scheduling methods not only contribute to a more efficient training process but also ensure fair improvements in accuracy across all clients. This addresses the challenges of personalized federated learning by ensuring that no single client's data disproportionately influences the global model.

References

- [1] IS Jacobs and CP Bean. Fine particles, thin films and exchange anisotropy (effects of finite dimensions and interfaces on the basic properties of ferromagnets). *Spin arrangements and crystal structure, domains, and micromagnetics*, 3:271–350, 1963.
- [2] A Mactaggert. The california privacy rights and enforcement act of 2020. *Retrieved October, 21(2020):19–0019*, 2019.

- [3] Brendan McMahan, Eider Moore, Daniel Ramage, Seth Hampson, and Blaise Aguera y Arcas. Communication-efficient learning of deep networks from decentralized data. In *Artificial intelligence and statistics*, pages 1273–1282. PMLR, 2017.
- [4] Tian Li, Anit Kumar Sahu, Manzil Zaheer, Maziar Sanjabi, Ameet Talwalkar, and Virginia Smith. Federated optimization in heterogeneous networks. *Proceedings of Machine learning and systems*, 2:429–450, 2020.
- [5] Sai Praneeth Karimireddy, Satyen Kale, Mehryar Mohri, Sashank Reddi, Sebastian Stich, and Ananda Theertha Suresh. Scaffold: Stochastic controlled averaging for federated learning. In *International conference on machine learning*, pages 5132–5143. PMLR, 2020.
- [6] Yoshua Bengio, Jérôme Louradour, Ronan Collobert, and Jason Weston. Curriculum learning. In *Proceedings of the 26th annual international conference on machine learning*, pages 41–48, 2009.
- [7] Saeed Vahidian, Sreevatsank Kadaveru, Woonjoon Baek, Weijia Wang, Vyacheslav Kungurtsev, Chen Chen, Mubarak Shah, and Bill Lin. When do curricula work in federated learning? In *Proceedings of the IEEE/CVF International Conference on Computer Vision*, pages 5084–5094, 2023.
- [8] Alysa Ziyang Tan, Han Yu, Lizhen Cui, and Qiang Yang. Towards personalized federated learning. *IEEE Transactions on Neural Networks and Learning Systems*, 2022.
- [9] Chelsea Finn, Pieter Abbeel, and Sergey Levine. Model-agnostic meta-learning for fast adaptation of deep networks. In *International conference on machine learning*, pages 1126–1135. PMLR, 2017.
- [10] Alex Nichol, Joshua Achiam, and John Schulman. On first-order meta-learning algorithms. *arXiv preprint arXiv:1803.02999*, 2018.
- [11] Daliang Li and Junpu Wang. Fedmd: Heterogenous federated learning via model distillation. *arXiv preprint arXiv:1910.03581*, 2019.
- [12] Yiqiang Chen, Xin Qin, Jindong Wang, Chaohui Yu, and Wen Gao. Fedhealth: A federated transfer learning framework for wearable healthcare. *IEEE Intelligent Systems*, 35(4):83–93, 2020.
- [13] Virginia Smith, Chao-Kai Chiang, Maziar Sanjabi, and Ameet S Talwalkar. Federated multi-task learning. *Advances in neural information processing systems*, 30, 2017.
- [14] Manoj Ghuhana Arivazhagan, Vinay Aggarwal, Aaditya Kumar Singh, and Sunav Choudhary. Federated learning with personalization layers. *arXiv preprint arXiv:1912.00818*, 2019.
- [15] Paul Pu Liang, Terrance Liu, Liu Ziyin, Nicholas B Allen, Randy P Auerbach, David Brent, Ruslan Salakhutdinov, and Louis-Philippe Morency. Think locally, act globally: Federated learning with local and global representations. *arXiv preprint arXiv:2001.01523*, 2020.
- [16] Liam Collins, Hamed Hassani, Aryan Mokhtari, and Sanjay Shakkottai. Exploiting shared representations for personalized federated learning. In *International conference on machine learning*, pages 2089–2099. PMLR, 2021.
- [17] Hong-You Chen and Wei-Lun Chao. On bridging generic and personalized federated learning for image classification. *arXiv preprint arXiv:2107.00778*, 2021.
- [18] Jaehoon Oh, Sangmook Kim, and Se-Young Yun. Fedbabu: Towards enhanced representation for federated image classification. *arXiv preprint arXiv:2106.06042*, 2021.